Flow boiling heat transfer and pressure drop characteristics of Isobutane in horizontal channels with twisted tapes

Alireza Sarmadian[a], Hadi Ahmadi Moghaddam[b], Amirmasoud Asnaashari[c], Hossein Ahmadi Nejad Joushani[d], Mostafa Moosavi[e], Mohammad S. Islam[f], Suvash C. Saha[f], Maziar Shafaee[g*]

[a]Department of Engineering and Design, University of Sussex, Brighton BN1 9QT, UK. Email: a.sarmadian@sussex.ac.uk

[b]Department of Mechanical Engineering, School of Engineering, University of Tasmania, Hobart, TAS 7001, Australia. Email: hadi.ahmadimoghaddamdastjerdi@utas.edu.au

[c]Renewable Energies Laboratory, Faculty of New Sciences and Technologies, University of Tehran, Tehran, Iran.

[d]School of Biomedical Engineering, University of Technology Sydney, NSW 2007, Australia.

[e]Department of Mechanical Engineering, Shiraz University, Shiraz, Iran.

[f]School of Mechanical and Mechatronic Engineering, University of Technology Sydney, NSW 2007, Australia.

[g]Faculty of New Sciences and Technologies, University of Tehran, Tehran, Iran.

[*]Corresponding author, Associate professor, Email: mshafaee@ut.ac.ir

Abstract

Using twisted tapes as a passive method for heat transfer improvement in a two-phase flow heat exchanger is experimentally studied. The test evaporator is a copper channel with a length of 1000 mm and an internal diameter of 8.1 mm which is installed horizontally. Three twisted tapes with twist ratios of 4, 10, and 15 are used at refrigerant vapor qualities in the range of 0.1-0.8 and refrigerant mass velocities between 160-350 $kgm^{-2}s^{-1}$. The natural refrigerant Isobutane (R600a) is chosen as the working fluid because it is environmentally friendly. According to the experiments, installing twisted tapes inside the channel augments both heat transfer rate and pressure drops over the plain channel. It is also observed that for both plain and twisted tape inserted channels, the values of heat transfer coefficients and pressure losses grow by giving rise to the refrigerant mass velocity and vapor quality. Results showed that the system performance factor varied

between 0.44-1.09 offering that using twisted tapes as a turbulator is beneficial under specific operating conditions. The empirical data showed that there is an optimum value of the working fluid mass velocity at which the performance of twisted tape inserted channels is higher.

Keywords: Heat transfer, Isobutane, Mass velocity, Pressure drop, Vapor quality

Nomenclature:

d	Tube diameter (mm)
G	Mass velocity ($kgm^{-2}s^{-1}$)
k	Thermal conductivity
PDR	Pressure drop ratio
PF	Performance factor
p	Pressure (kPa)
x	Vapor quality

Greek symbols

ε	Zivi void fraction
μ	Viscosity
ρ	Density
γ	Efficiency of the evaporator insulation

Subscripts

eva	Evaporator
f	Liquid phase
fric	Frictional
g	Vapor phase
i	Inner
lat	Latent
mom	Momentum
o	Outer
p	Plain
pe	Pre-evaporator
ref	Refrigerant
s	Smooth
sat	Saturated
sen	Sensible

tot	Total
ts	Test section
w	Wall
wat	Water

1. Introduction

With the growth of the population worldwide and the industrialization of countries, global warming has become a concern. Therefore, using environmentally friendly refrigerants in various refrigeration and HVAC systems is indispensable. The refrigeration and HVAC systems have had a considerable impact on global warming. These systems were responsible for 7.8% of overall greenhouse gas emissions in 2014 [1]. Taking into account the two prominent environmental concerns of refrigerants (ozone depletion potential (ODP) and global warming potential (GWP)), employing natural refrigerants is attractive as these fluids have a relatively small GWP with an ODP of zero [2].

Refrigerant R600a (Isobutane) is a natural hydrocarbon that exhibits favorable thermodynamic characteristics. R600a is obtainable in nature and is cheap. It is also easy to mix and use with common materials, nano-fluids, and lubricants [3, 4]. Therefore, this refrigerant has been a matter of attention in several studies. In this regard, Sempertegui-Tapia and Ribatski [5] empirically explored the evaporative heat transfer performance of several environmentally friendly refrigerants including R600a, R1234yf, and R1234ze(E) to replace the traditional refrigerant R134 considering different operating conditions. Their experiments illustrated that while the obtained heat transfer coefficients using R600a were smaller than those of the other fluids for vapor qualities below 0.2, the heat transfer rates significantly improved using this refrigerant over the other cases by increasing the vapor quality. Alimardani et al. [6] studied the forced convective evaporation of R600a in tube heat exchangers equipped with spiral coils. Their study showed that the spiral coils usage contributes to the heat transfer enhancement over the smooth tubes. It was also demonstrated that spiral coil inserts affect the transition of flow regimes. Shafaee et al. [7-9] examined boiling and condensation of R600a in horizontal plain and dimpled channels. It was observed that using channels with enhanced surfaces increases the heat transfer coefficient up to 200% for both regimes. However, the pressure drops of the modified channels also increased up

to 103% for the flow boiling and 195% for the flow condensation, compared to the plain case. In another piece of research carried out by Yang et al. [10], the pressure loss and heat transfer rates of R600a and R1234ze(E) were obtained and compared during evaporation inside a horizontal pipe under different values of mass velocity, saturation pressure, and heat flux. The experimental results showed that using R600a yielded higher rates of transferred heat and pressure drop. Within other experimentally performed studies by Moghaddam et al. [11, 12] on condensation of R600a in horizontal channels with wire coil inserts, it was observed that installing inserts augments the amount of heat transfer coefficients up to 107% over the plain test case. However, the wire coils usage also resulted in an increase in pressure drop. The pressure drop of the wire coil installed channels was 1.51 to 11.97 times of that of the plain channel, depending on the type of inserts and system operating conditions. Their empirical data also showed that heat transfer rates and pressure losses grow as the refrigerant mass velocity and vapor quality increase.

In addition to the environmental aspects, decreasing energy usage in refrigeration systems is of high interest. Employing twisted tape inserts in heat exchangers for boosting the rate of transferred heat is considered an attractive technique as producing these inserts is easy and cost-effective. Furthermore, installing these devices inside tube heat exchangers is convenient. As reported by Kanizawa et al. [13] and Shishkin et al. [14], twisted tapes usage gives rise to the heat transfer in heat exchangers by providing a swirling and turbulent flow, although a pressure loss penalty is inevitable. During another piece of experimental research, Akhavan-Behabadi et al. [15] illuminated the impacts of installing twisted tapes with twist ratios between 6 to 15 inside tube heat exchangers during forced convective evaporation of R134a. Through the investigation, it was observed that installing twisted tapes inside the tube heat exchangers augments the pressure drops up to 180%, and heat transfer coefficients up to 57% over the smooth test case. Similarly, Hejazi et al. [16] investigated the influences of installing twisted tapes with twist ratios in the range of 6 to 15 during forced convective condensation of R134. They observed an augmentation in both heat transfer coefficients and pressure drops when the inserts were utilized. The best performance was observed by using an insert with a twist ratio of 9. In two other investigations, Salimpour and Yarmohammadi [17, 18] explored the performance of tube heat

exchangers equipped with twisted tape inserts during condensation of R404A. Salimpour and Yarmohammadi [17, 18] reported that the pressure losses and heat transfer coefficients in the pipes with inserts increased up to 239% and 50%, respectively. However, it is noticeable that the mentioned studies [13-18] were conducted with R134a (with a GWP of 1300) and R404A (with a GWP of 3922) refrigerants which are not environmentally friendly working fluids. Recently, Moghaddam et al. [19] explored the performance of horizontal tube heat exchangers with twisted tape inserts during the boiling of R600a. Their results showed that installing twisted tapes raises both heat transfer and pressure drops simultaneously resulting in system performance factors between 0.39 to 1.05. They observed that the system performance factor relies on different parameters including refrigerant mass velocity, vapor quality, and geometry of inserts. More discussions regarding the performance of twisted tape inserts in heat exchangers are provided by Kumar et al. [20], Bucak and Yilmaz [21], Dewan et al. [22], Liu and Sakr [23], and Garg et al. [24].

In this experimental research, the heat transfer and pressure loss features of a horizontally installed channel are investigated during the boiling of R600a. Furthermore, three twisted tape inserts with various twist ratios are used to illuminate the impact of using these instruments on the system performance. It is worthy of note that no investigations presented previously do either of the following:

- Evaluate the heat transfer characteristics of R600a in horizontal twisted tape inserted channels.
- Evaluate the pressure drop characteristics of R600a in horizontal twisted tape inserted channels.

In the following sections of the present paper, the experimental setup is explained and the equations for calculating the heat transfer and pressure loss data are presented. In the next step, the obtained heat transfer data for both cases (plain channel and twisted tape installed channel) is provided. The pressure drop data is also presented for both cases. The results related to the heat transfer coefficient and pressure drop of the plain channel are compared with some correlations developed in previous studies. Finally, by computing the system performance

factor, the effectiveness of the twisted tapes under different operating conditions is explored.

2. Experimental setup

The overall view of the test cycle and the twisted tape installed test channel is shown in Fig. 1. A circular cross-section channel made from copper (alloy C10300 with thermal conductivity of 385.7 $Wm^{-1}K^{-1}$) with a length of 1000 mm, an inner diameter of 8.1 mm, and a wall thickness of 0.71 mm is considered as the test evaporator. Furthermore, three twisted tape inserts made from aluminum (grade 6063 with thermal conductivity of 201 $Wm^{-1}K^{-1}$) with a length of 1000 mm and different twist ratios are installed in the full length of the test section and tested. Therefore, there is no distance between the insert and the test section inlet and outlet. The twist ratio is defined as the ratio of the insert pitch to the channel inner diameter. Table 1 presents the physical dimensions of the inserts.

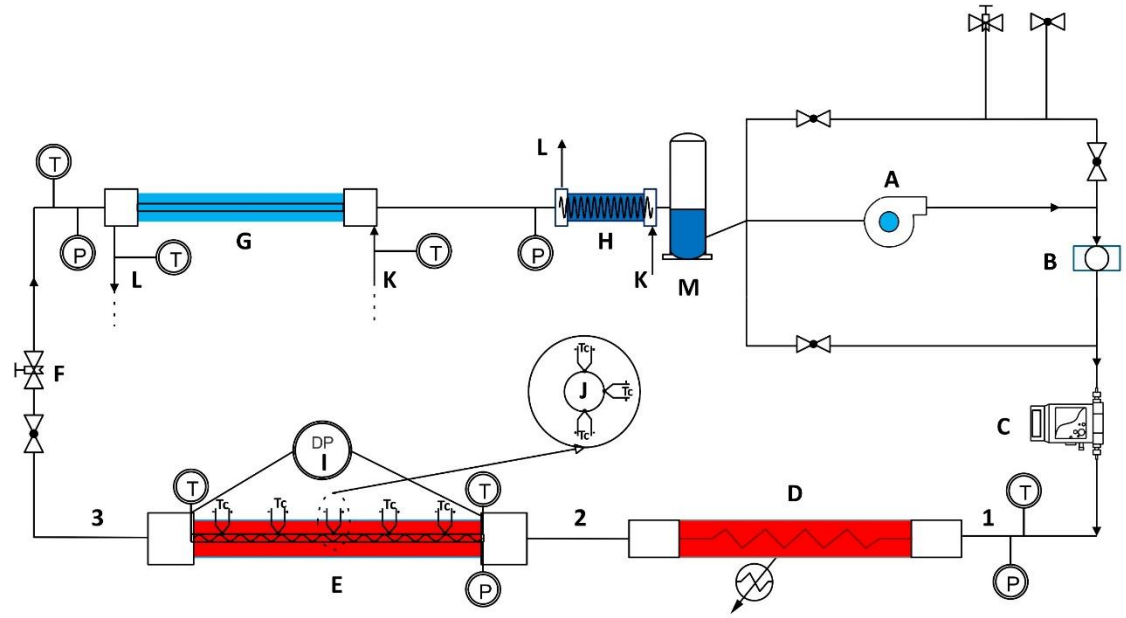

A- Pump	E- Test Evaporator	I- Differential Pressure Transmitter	M- Separator Tank	Tc - Thermocouple
B- Sight Glass	F- Needle Valve	J- Cross-section Evaporator	1- Heater inlet	(P) - Pressure
C- Flow meter	G- Condenser	K- Water inlet	2- Evaporator inlet	(T) - Temperature
D- Heater	H- Post Condenser	L- Water outlet	3- Evaporator outlet	

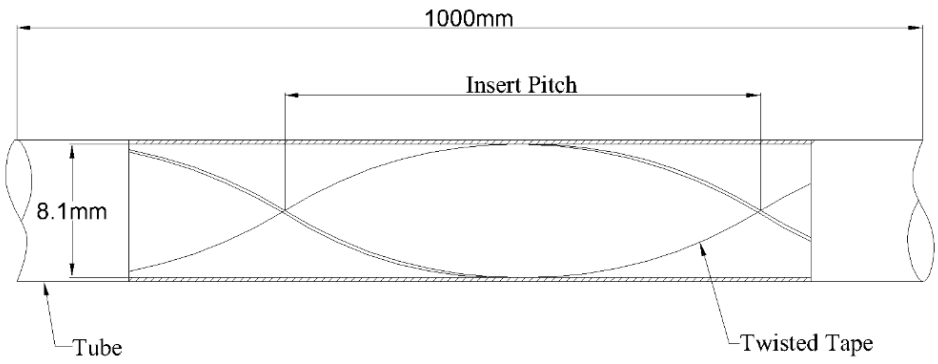

Fig. 1. The schematic view of the current test cycle and twisted tape installed channel.

Table 1. The physical dimensions of the twisted tapes.

Tube set	Tube inner diameter (mm)	Twist ratio
Plain	8.1	-
TT1	8.1	15
TT2	8.1	10
TT3	8.1	4

To record the values of temperature along the test channel, temperature sensors are attached to the test section wall in five positions, with a distance of 200 mm from each other. In each position, three sensors are welded to the bottom, top, and side of the tube. Their mean value is considered for calculations. Temperature and pressure sensors are attached to different points of the cycle. A condenser is also utilized in the cycle which employs water as the coolant for condensing R600a. A post-condenser is also installed after the main condenser to ensure that the refrigerant flow entering the pump is in the liquid state. To circulate the coolant water and refrigerant in their loops, variable frequency gear pumps are employed in each loop. The measuring of the mass flow rate of the refrigerant and water is carried out by means of two mass flow meters. Furthermore, a differential pressure drop transducer measures the total pressure drop in the length of the test evaporator. An electrical heater is installed prior to the test channel to attain the required vapor quality at the entrance of the test channel. In terms of reducing heat loss from the test section to the surrounding area, insulation is used. The

insulation materials used in this experiment are flame retardant glass fiber tape with a thermal conductivity of 0.05 $Wm^{-1}K^{-1}$, glass wool with a thermal conductivity of 0.04 $Wm^{-1}K^{-1}$, and foam insulation with a thermal conductivity of 0.02 $Wm^{-1}K^{-1}$. Further information regarding the instruments used in the current cycle is provided in Table 2.

Table 2. The utilized devices in the present test cycle.

Instrument	Model	Accuracy
Gear pump	ZDF, Czech	-
Temperature sensor (attached to test tube)	T-type	0.1 K
Pressure gauge	EN 837-1 Wika	1kPa
Differential pressure drop transducer	PDM 75	0.075% of full scale (0.69-15.4 kPa)
Temperature sensor (inlet and outlet)	RTD PT 100	0.1 K
Data logger	Lutron 4208 SD	-
Coriolis mass flow meter	Mass/2100/6000 Danfoss, Denmark	0.1% of full scale (31-67.7 kgh^{-1})

In order to perform the tests, a wide range of the refrigerant vapor quality (between 0.1-0.8) and mass velocities (between 160-350 $kgm^{-2}s^{-1}$) are considered. Further information on the operating conditions of the study is presented in Table 3.

Table 3. Operating parameters of the present study.

Parameter	Type or value	Unit
Refrigerant	Isobutane (R600a)	-
Refrigerant mass flux	160, 200, 300, and 350	$Kgm^{-2}s^{-1}$
Refrigerant Reynolds number	9840, 13270, 18900, and 24870	-
Prandtl number	3.7	-
Average pressure	4.9	bar
Saturation temperature	310.15	K
Vapor quality	0.1-0.8	-
Pressure drop	0.69-15.4	kPa

3. Data reduction

3.1. Heat transfer coefficient (HTC)

The quasi-local heat transfer coefficient of the test evaporator is computed based on the following equation [7]:

$$\frac{1}{h_{ref}} = \frac{T_{wall} - T_{sat}}{q_x} - \frac{\ln\left({}^{d_{out}}/_{d_{inner}}\right) d_{inner}}{2k} \quad (1)$$

In Eq. (1), T shows the temperature based on the mean of temperature recordings, and d presents the channel diameter. q_x and k demonstrate the heat flux and thermal conductivity, respectively.

The refrigerant vapor quality is determined using the mean of vapor quality at the inlet and outlet of the test channel. The vapor quality at the channel inlet is computed using the following relation [7]:

$$x_{in} = \frac{Q_{t,pe} - C_p \dot{m}_{ref}(T_{sat,pe} - T_{ref,pe,in})}{\dot{m}_{ref} h_{fg,pe}} \quad (2)$$

$$Q_{t,pe} = \gamma (VI)_{pe} = Q_{sens} + Q_{lat} \quad (3)$$

$$Q_{sens} = C_p \dot{m}_{ref}(T_{sat,pe} - T_{ref,pe,in}) \quad (4)$$

$$Q_{lat} = \dot{m}_{ref} h_{fg,pe} x_{in} \quad (5)$$

$$\gamma = \dot{m}_{ref}(h_3 - h_1) / (VI)_{pe} + (VI)_{ts} \quad (6)$$

The vapor quality at the outlet of test channel is obtained by the following:

$$x_{out} = x_{in} + \gamma (VI)_{ts} / h_{fg,ts} \quad (7)$$

Where V and I demonstrate the electric voltage and current, respectively. $Q_{t,pe}$ shows the overall transferred heat in the pre-evaporator. Q_{sens} and Q_{lat} represent the sensible and latent heat, respectively. C_p is the specific heat of the refrigerant. $h_{fg,ts}$ and $h_{fg,pe}$ also show the vaporization enthalpy of the test section and pre-evaporator, respectively. γ represents the efficiency of the explored test evaporator insulation, which was found to be about 0.95.

3.2. Frictional pressure drops

The overall pressure drop in the test evaporator is measured by the pressure drop transducer. The measured pressure drop is equal to the summation of three components, exhibited as the following:

$$\Delta P_{tot} = \Delta P_{mom} + \Delta P_{fri} + \Delta P_{sta} \quad (8)$$

Where ΔP_{mom}, ΔP_{fri}, ΔP_{sta} are momentum pressure loss, frictional pressure loss, and static pressure loss, respectively. Since the test channel is located horizontally, the amount of the latter term in Eq. (8) is zero.

To calculate the momentum pressure loss, Eq. (9) is taken into account [25]:

$$\Delta P_{mom} = G_{tot}^2 \left\{ \left[\frac{(1-x)^2}{\rho_l(1-\varepsilon)} + \frac{x^2}{\rho_g \varepsilon} \right]_{out} - \left[\frac{(1-x)^2}{\rho_l(1-\varepsilon)} + \frac{x^2}{\rho_g \varepsilon} \right]_{in} \right\} \quad (9)$$

Where x, G, ρ, and ε are refrigerant vapor quality, mass flux, density, and void fraction, respectively.

The suggested formula by Zivi [26] is utilized for calculating the void fraction:

$$\varepsilon = \frac{1}{1 + \left(\frac{1-x_{te}}{x_{te}}\right)\left(\frac{\rho_g}{\rho_l}\right)^{2/3}} \quad (10)$$

By subtracting the momentum pressure loss from the overall pressure loss, the frictional pressure loss is achieved.

To illuminate the uncertainties in the calculation of different parameters, a proposed scheme by Schultz and Cole is utilized [27]. The obtained uncertainties are provided in Table 4.

Table 4. Uncertainties of different parameters obtained in this study.

Parameter	Uncertainty	Units
Momentum pressure drop	±18.4%	Pa
Frictional pressure drop	±2.85%	Pa
Refrigerant mass flux	±12.4%	$kgm^{-2}s^{-1}$
Void fraction	±2.3%	-
Vapor quality	±5%	-
Heat transfer coefficient	±8%	$Wm^{-2}K^{-1}$
Performance factor	±4.3%	-

3.3. Performance factor (PF)

To inspect the impacts of inserts on the cycle performance and illuminate their effectiveness, a parameter named performance factor (PF) is utilized. PF is calculated according to the following relation [28]:

$$PF = \frac{(W/_{HTC})_p}{(W/_{HTC})_r} = \frac{HTC_r/_{HTC_p}}{(\Delta P)_r/_{(\Delta P)_p}} = R_{HTC}/_{R_{\Delta P}} \quad (11)$$

In the above-mentioned equation, $(W/_{HTC})_p$ represents the ratio of pump consumed power to HTC for the case of the plain channel. $(W/_{HTC})_r$ shows the same ratio for the case of rough channels (twisted tape inserted channels). The utilization of inserts is advantageous if PF is larger than one.

Another parameter entitled pressure drop ratio (PDR) is defined as:

$$PDR = \frac{(\Delta P)_r}{(\Delta P)_p} \quad (12)$$

PDR shows the ratio of pressure drops in twisted tape inserted channels to the smooth channel. This parameter will be used in the next sections for elaborating on the trend of performance factor.

4. Results and discussions

In this section, the HTC and pressure drop results are presented for both plain and channels with inserts. Furthermore, to investigate the accuracy of the obtained data, the HTC and pressure loss results for the smooth test case are compared with the previous correlations in the literature. Finally, the cycle performance factor is determined using different inserts.

4.1. Heat transfer coefficient (HTC)

By comparing the distribution of HTC data for both smooth and twisted tape installed channels in Fig. 2, it is observed that utilizing these inserts significantly augments the HTC for all mass fluxes and vapor qualities. Indeed, the inserts usage augments the flow turbulence and interrupts the development of the laminar sub-layer. Therefore, the heat transfer rate increases. The results also show that the

smaller the twist ratio, the higher the HTC growth. The reason could be that the swirling flow and turbulence become stronger as the insert pitch decreases.

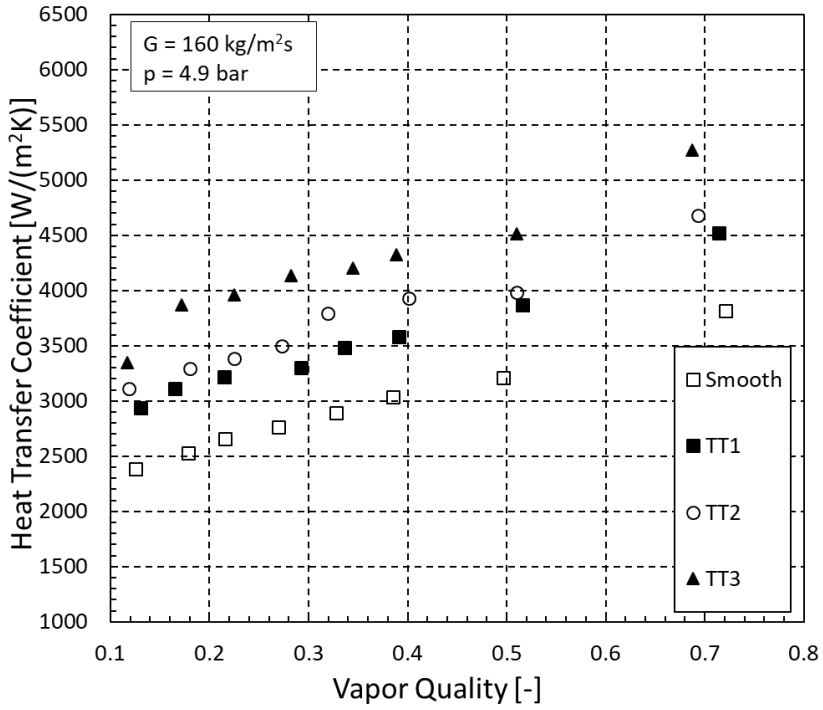

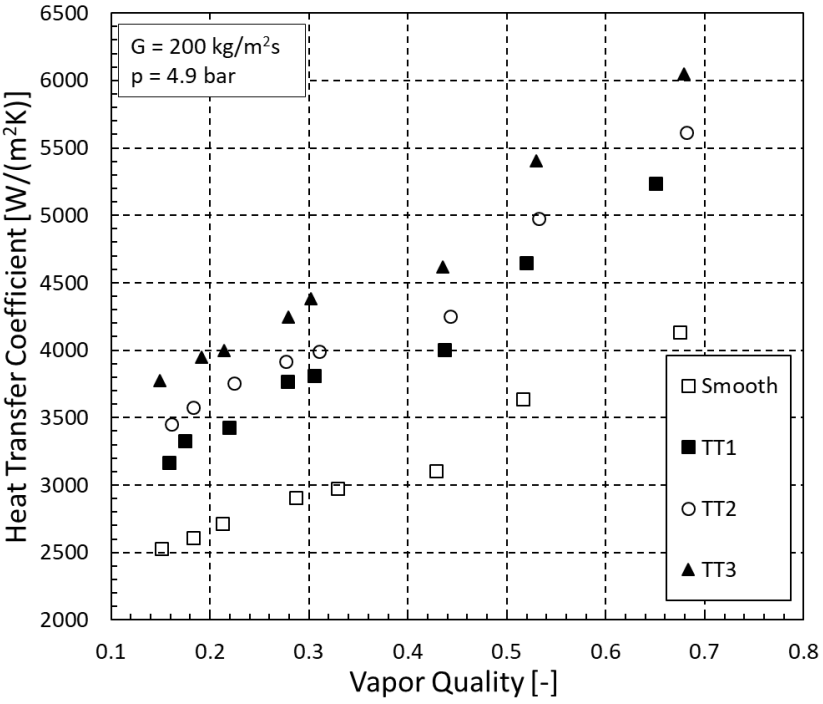

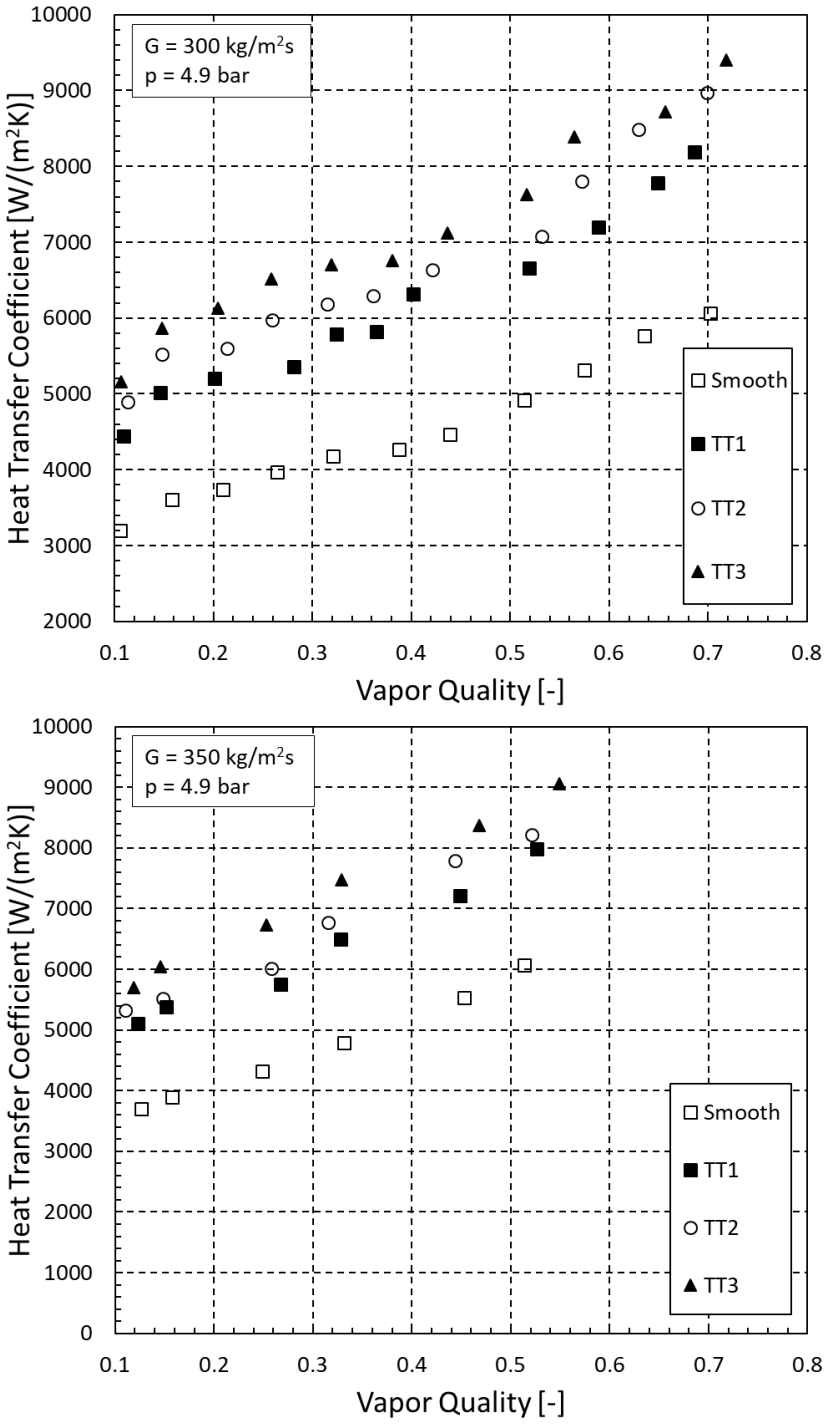

Fig. 2. The variations of the obtained heat transfer coefficients with vapor quality under different mass fluxes.

It is also deducible from Fig. 2 that the amounts of HTC in both smooth and twisted tape installed channels increase by giving rise to the value of vapor quality and mass velocity. When the refrigerant vapor quality is low, there exists a thinner layer of liquid refrigerant film on the channel's inner surface which in turn yields lower thermal resistance. Therefore, HTC increases. Regarding the impacts of mass

velocity increment, it should be noted that when the mass velocity increases, the convection and flow turbulence augment, yielding higher values of HTC.

The current HTC results for the plain channel are compared with the correlation of Kattan-Thome-Favrat [29] to evaluate the consistency of the experimental results. As observed in Fig. 3, the HTC data points are predicted by this correlation in the error range of -20% to +25%. This model is proposed based on the flow patterns for the prediction of heat transfer coefficients during flow boiling inside horizontal channels.

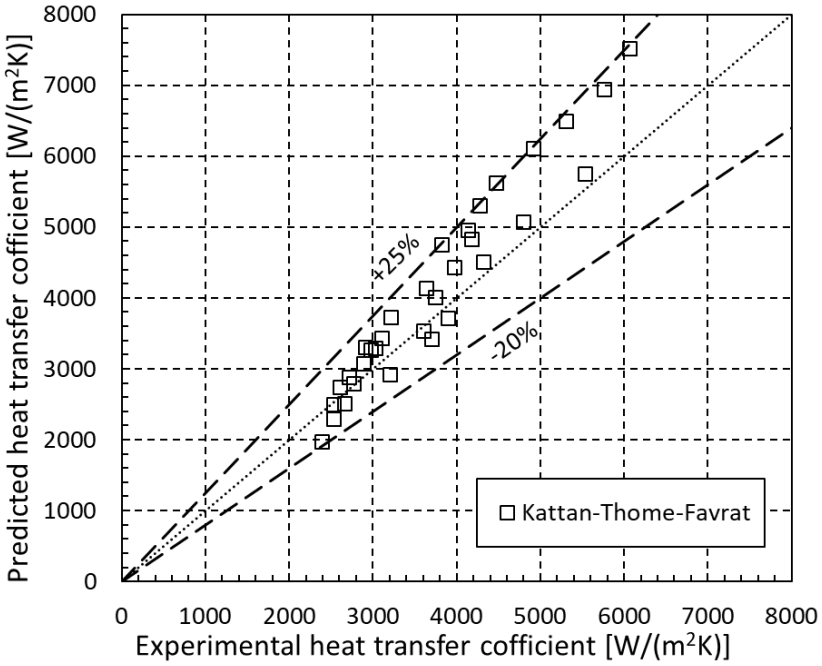

Fig. 3. The comparison between the heat transfer coefficients obtained by the correlation of Kattan-Thome-Favrat [29] and current experiments.

4.2. Frictional pressure drops

As the refrigerant vapor quality varies, the changes of frictional pressure losses in the plain and twisted tape inserted channels are presented for different mass fluxes in Fig. 4. It is shown that larger levels of loss are imposed on the system by installation of the twisted tapes. By inserting the twisted tapes, the frictional surface within the channel increases. Therefore, the frictional losses between the flow and the inserts increase the pressure drops. The other possible ground could

be that by installing the inserts, there exists a smaller cross-sectional area for the refrigerant flow. By the reduction of area, the velocity of flow increases, which yields higher losses. The other observation is that under all operating conditions, the pressure drops augment by reducing the twisted tape pitch or twist ratio. The reason for this is that when an instrument with a smaller pitch is employed, the frictional surface per length of the channel increases. Therefore, pressure losses grow. Furthermore, inserts with a smaller twist ratio induce more turbulence to the flow. Thus, by increasing the turbulence intensity the pressure losses rise.

It is observable in Fig. 4 that for all smooth or rough test cases the values of pressure losses grow as the refrigerant vapor quality augments. As explained in previous studies [12, 16, 30], the vapor refrigerant volume inside the channel rises by increasing the refrigerant vapor quality. Therefore, the vapor refrigerant velocity augments, yielding a larger velocity difference between the vapor and liquid phases. Consequently, the shear stresses between the vapor and liquid refrigerant and pressure losses grow. Fig. 4 also illustrates that the values of pressure losses rise with the refrigerant mass velocity increment. Stronger shear stress would be generated between the flow and the twisted tape inserts surface as well as the tube inner surface by raising the mass flux. Furthermore, the flow in twisted tape installed channels has higher turbulence intensity, due to the presence of inserts which results in larger shear stresses. Therefore, the values of pressure drops augment.

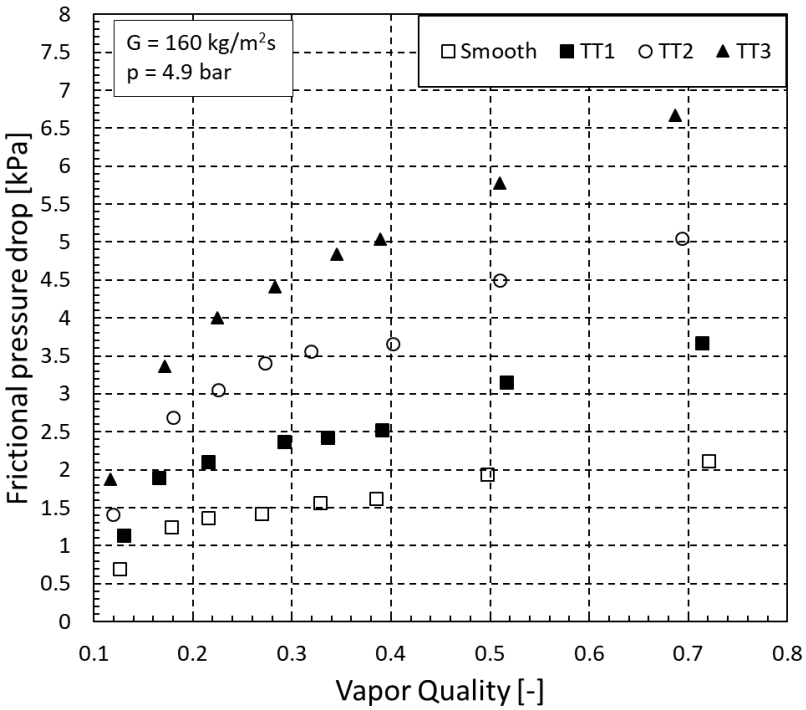
G = 160 kg/m²s
p = 4.9 bar
Smooth
TT1
TT2
TT3
Frictional pressure drop [kPa]
Vapor Quality [-]
0
0.5
1
1.5
2
2.5
3
3.5
4
4.5
5
5.5
6
6.5
7
7.5
8
0.1
0.2
0.3
0.4
0.5
0.6
0.7
0.8

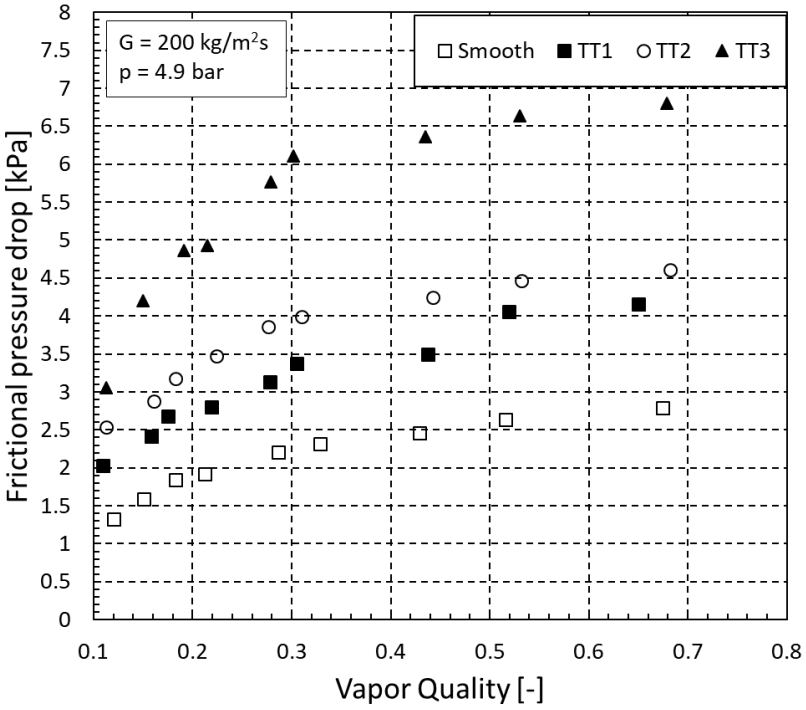
G = 200 kg/m²s
p = 4.9 bar
Smooth
TT1
TT2
TT3
Frictional pressure drop [kPa]
Vapor Quality [-]
0
0.5
1
1.5
2
2.5
3
3.5
4
4.5
5
5.5
6
6.5
7
7.5
8
0.1
0.2
0.3
0.4
0.5
0.6
0.7
0.8

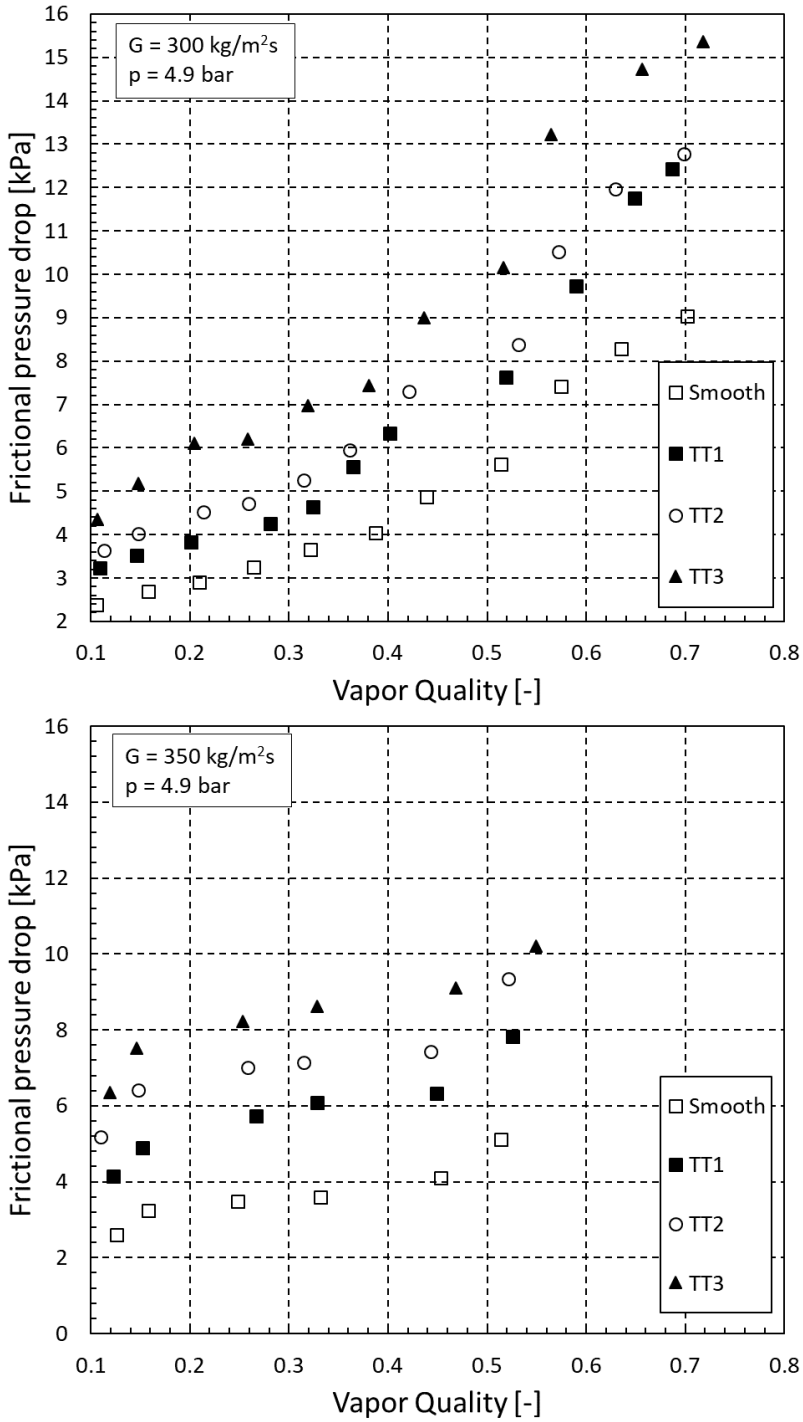

Fig. 4. The variations of the obtained pressure losses with vapor quality under different mass fluxes.

The experimentally obtained pressure drop results for the plain channel are compared to the results predicted by the correlations of Friedel [31] and Muller-

Steinhagen and Heck [32]. As can be observed in Fig. 5, these correlations predict the data within an error window between -25% to +30%.

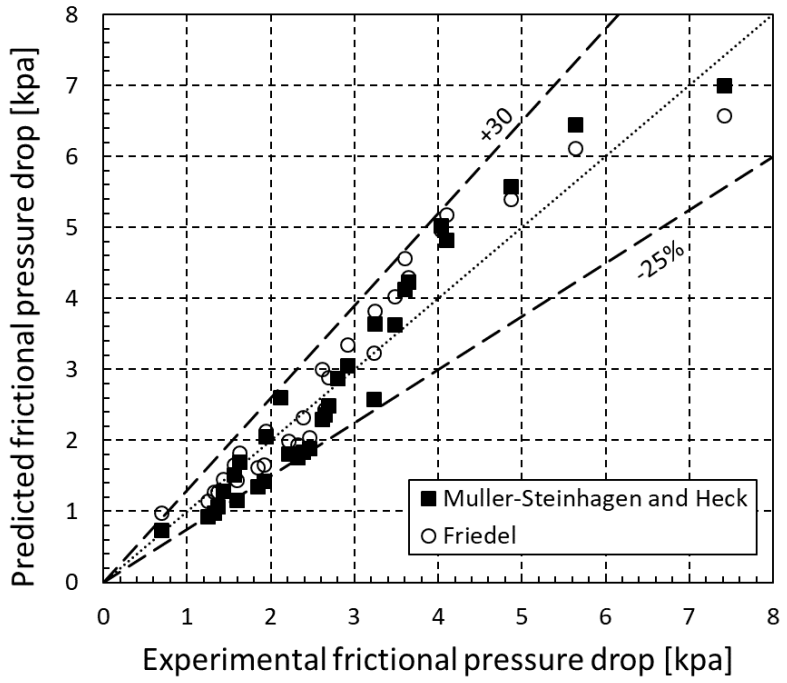

Fig. 5. A comparison between the plain channel pressure drop results obtained using the correlations of Friedel [31] and Muller-Steinhagen and Heck [32].

4.3. Performance factor (PF)

As observed in previous sections, the values of both pressure drops and HTC augment simultaneously with installation of twisted tapes. The increased HTC is desirable but increased pressure drop is not desirable, since it increases the power consumed by the pump for circulating the refrigerant. Therefore, the performance factor illuminates the usefulness of the twisted tape inserts.

Fig. 6 depicts the obtained values of the performance factors at different mass fluxes and vapor qualities. As observed, generally, PF grows by increasing the mass flux from 160 $kgm^{-2}s^{-1}$ and reaches higher values at 300 $kgm^{-2}s^{-1}$. However, a reverse trend is seen by increasing the mass flux beyond 300 $kgm^{-2}s^{-1}$. To understand the reasons behind this trend, Fig. 7 is provided. This plot presents the ranges of changes in the pressure drop ratio of the rough channels to the plain channel. As can be seen, PDR is reduced by augmenting the mass flux up to 300

$kgm^{-2}s^{-1}$. The plot shows that the effects of inserts at lower mass fluxes are considerable. As the mass flux rises, the effects of inserts gradually fade because the impacts of momentum pressure drop, a result of the increased refrigerant velocity, becoming significant. Similar observations were reported by Naulboonrueng et al. [33] and Alimardani et al. [30], who concluded that employing modified surfaces and inserts at lower refrigerant mass fluxes results in higher pressure drop increments over the plain channel. However, as illustrated in Fig. 7, PDR gradually augments as the mass flux increases from 300 to 350 $kgm^{-2}s^{-1}$. By further increment of the mass flux, the effects of shear stress between the flow and channel inner wall as well as the surface of the inserts become significant due to the increased flow velocity.

Distribution of data in Fig. 6 shows a nonmonotonic behavior of PF. The value of performance factor is a function of two parameters, including heat transfer and pressure drop in both smooth and twisted tape inserted tubes. As discussed by Macdonald and Garimella [34], (who studied the condensation of propane in tubes), forced convective condensation or evaporation is a severely unstable and fully-turbulent phenomenon, since the vapor phase and liquid phase flow together, accompanied by transformation of phases. For coiled wire inserted tubes, this phenomenon is worsened, resulting in increased complexity and turbulence of flow. Due to this, the values of heat transfer and pressure drops have severely nonlinear behavior, resulting in the nonmonotonic trend of the performance factor. It is worth noting that similar observations regarding the nonlinear and nonmonotonic behavior of heat transfer, pressure drop, or performance factor results in two-phase flow systems are reported in previous studies [12, 19].

Fig. 6 also shows that the tube set “TT1” with the twist ratio of 15 presents the best performance as compared to the other inserts. Depending on the type of utilized inserts and the operating conditions of the cycle, the cycle performance factor varied between 0.44-1.09. The best performance is obtained by “TT1” at the mass flux of 300 $kgm^{-2}s^{-1}$ and the vapor quality of 0.32.

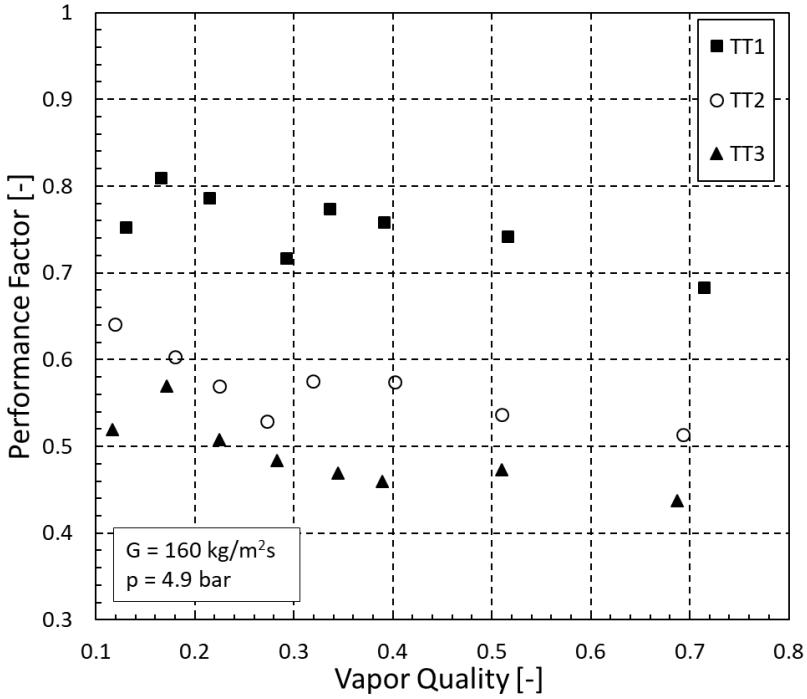
TT1
TT2
TT3
G = 160 kg/m²s
p = 4.9 bar
Performance Factor [-]
Vapor Quality [-]
1
0.9
0.8
0.7
0.6
0.5
0.4
0.3
0.1
0.2
0.3
0.4
0.5
0.6
0.7
0.8

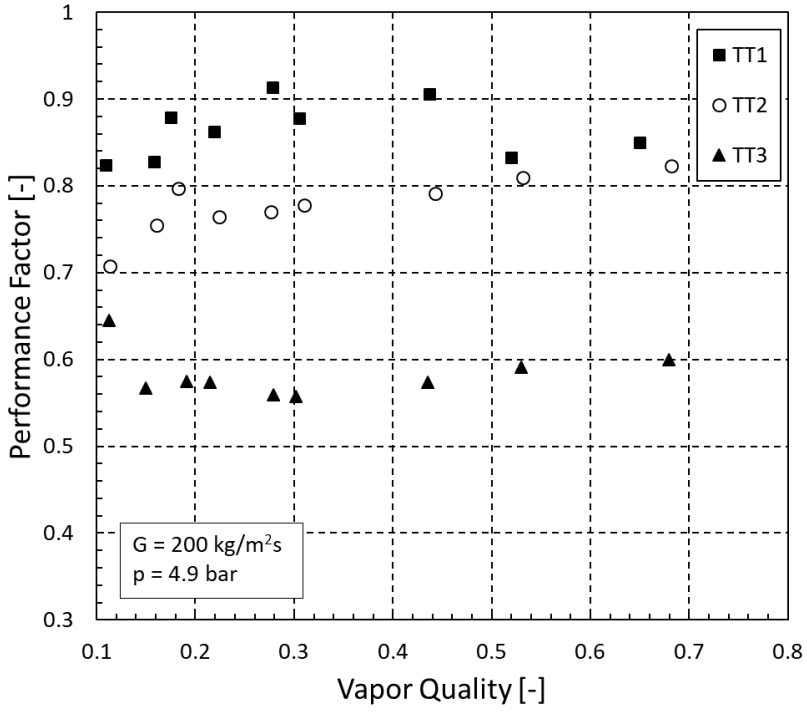
TT1
TT2
TT3
G = 200 kg/m²s
p = 4.9 bar
Performance Factor [-]
Vapor Quality [-]
1
0.9
0.8
0.7
0.6
0.5
0.4
0.3
0.1
0.2
0.3
0.4
0.5
0.6
0.7
0.8

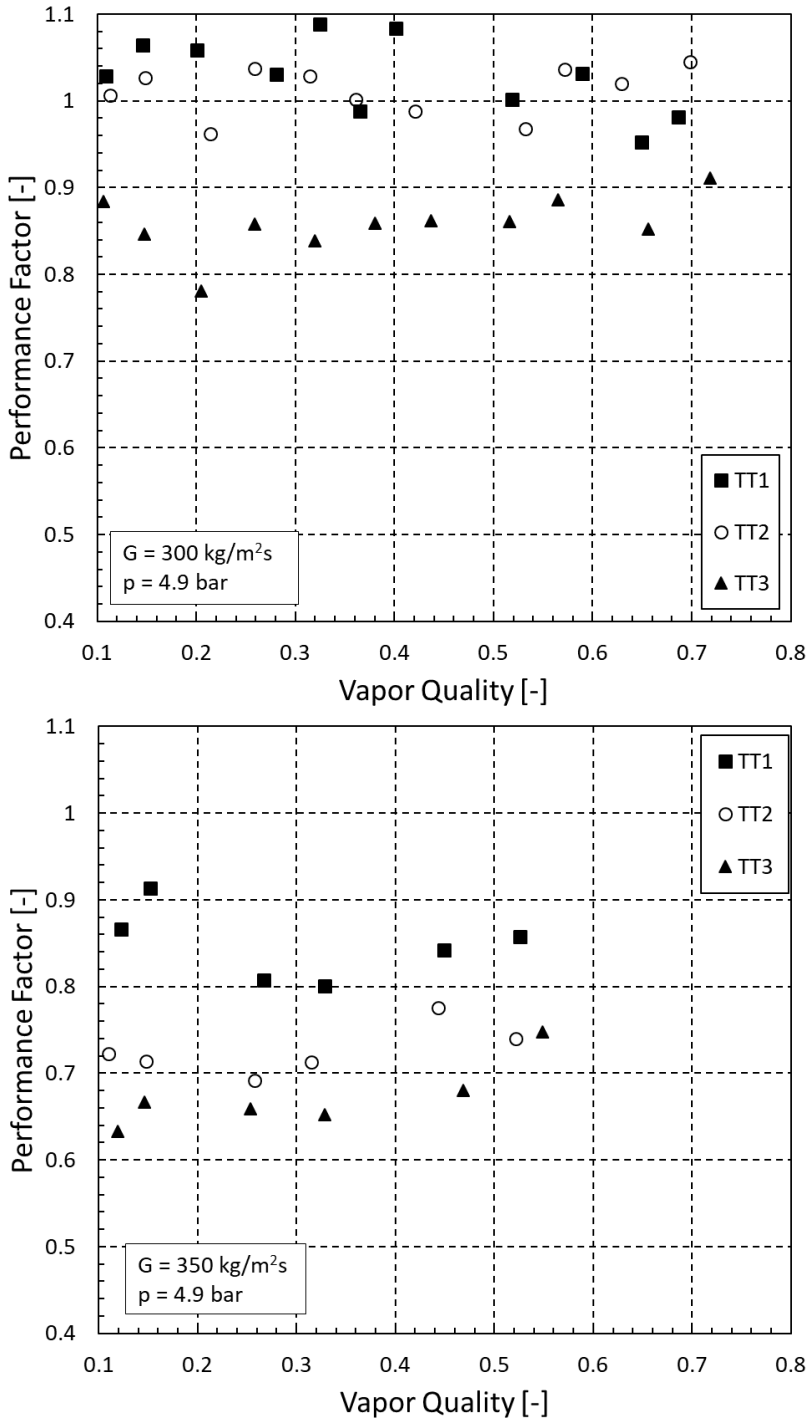

Fig. 6. The values of system performance factor using different inserts under various vapor qualities and mass velocities.

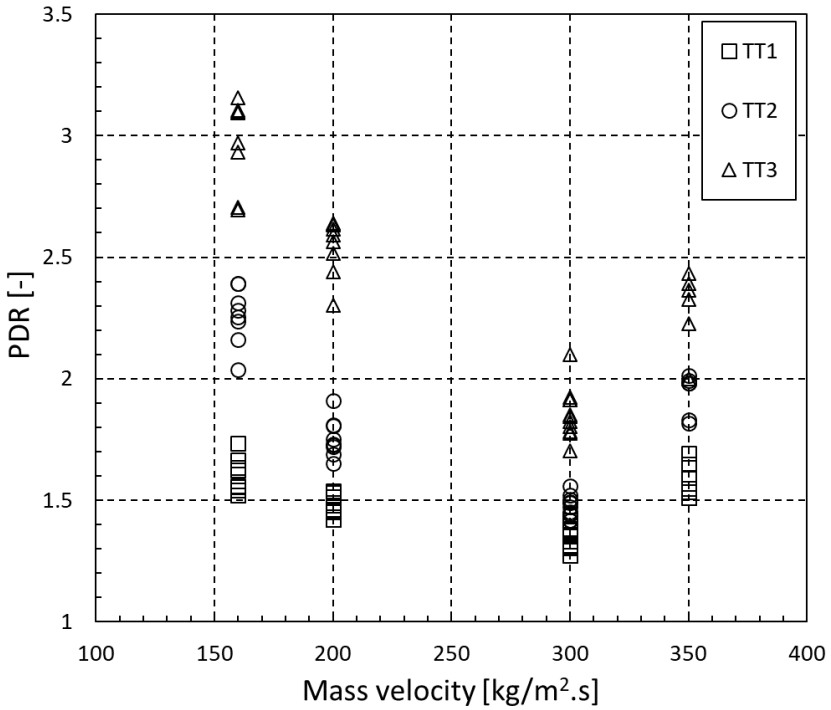

Fig. 7. The ranges of pressure drop ratios of the twisted tape inserted channels to the plain channel.

5. Conclusions

An empirical setup is constructed for determining the impact of using twisted tape inserts on the thermal performance of horizontal channels during the boiling of Isobutane. The experiments are conducted for refrigerant vapor qualities in the range of 0.1-0.8, and mass velocities in the range of 160-350 $kgm^{-2}s^{-1}$. Three inserts with twist ratios of 4, 10, and 15 are utilized for enhancing the heat transfer rate. The following conclusions are drawn based on the obtained data:

- Employing twisted tapes simultaneously increases the heat transfer rate and pressure drops of R600a flow boiling in comparison to the plain test channel.
- For both plain and twisted tape inserted channels, the values of HTC and pressure losses rise by increasing the vapor quality and mass velocity.
- The pressure loss ratios of the twisted tape installed channels to the plain channel are generally larger at lower mass velocities.
- For the refrigerant mass velocity, there is an optimum point at which the cycle performance factor is higher in twisted tape inserted channels.

- The calculated performance factors of the cycle using inserts were in the range of 0.44-1.09.

The present research shows that using twisted tapes in horizontal two-phase flow heat exchangers is advantageous under specific operating conditions. If the primary concern is to augment the heat transfer rate and the increased consumed power by the pump is justifiable, using twisted tapes is recommended for a wide range of operating conditions.

6. Declaration of competing interests:

None.

7. Appendix (calculation of uncertainties)

To determine the uncertainty of different parameters in this study, a method proposed by Schultz and Cole [27] is used.

For the frictional pressure drop, we have:

$$\Delta P_{fric} = \Delta P_{tot} - \Delta P_{mom}$$

According to Schultz and Cole [27]:

$$U_R = \left[\sum_{i=1}^{n} \left(\frac{\partial R}{\partial V_i} U_{V_i}\right)^2\right]^{\frac{1}{2}}$$

Therefore,

$$U_{\Delta P_{fric}} = \left[\left(U_{\Delta P_{tot}}\right)^2 + \left(U_{\Delta P_{mom}}\right)^2\right]^{1/2}$$

Based on the uncertainty of pressure drop transducer listed in Table 2:

$$U_{\Delta P_{tot}} = 0.00075$$

Considering Eq. (9), we have:

$$\Delta P_{mom} = G_{tot}^2 \left\{\left[\frac{(1-x)^2}{\rho_l(1-\varepsilon)} + \frac{x^2}{\rho_g \varepsilon}\right]_{out} - \left[\frac{(1-x)^2}{\rho_l(1-\varepsilon)} + \frac{x^2}{\rho_g \varepsilon}\right]_{in}\right\}$$

Therefore:

$$U_{\Delta P_{mom}} = \left[\left(\frac{\partial \Delta P_{mom}}{\partial G} U_G\right)^2 + \left(\frac{\partial \Delta P_{mom}}{\partial x} U_x\right)^2 + \left(\frac{\partial \Delta P_{mom}}{\partial \varepsilon} U_\varepsilon\right)^2\right]^{\frac{1}{2}}$$

After derivation, we have:

$$U_{\Delta P_{mom}} = \left[\left(2GU_G\left\{\left[\frac{(1-x)^2}{\rho_l(1-\varepsilon)} + \frac{x^2}{\rho_g\varepsilon}\right]_{out} - \left[\frac{(1-x)^2}{\rho_l(1-\varepsilon)} + \frac{x^2}{\rho_g\varepsilon}\right]_{in}\right\}\right)^2 + \left(G_{tot}^2\left\{\left[\frac{-2xU_x}{\rho_l(1-\varepsilon)} + \frac{2xU_x}{\rho_g\varepsilon}\right]_{out} - \left[\frac{-2xU_x}{\rho_l(1-\varepsilon)} + \frac{2xU_x}{\rho_g\varepsilon}\right]_{in}\right\}\right)^2 + \left(G_{tot}^2\left\{\left[\frac{(1-x)^2U_\varepsilon}{\rho_l(1-\varepsilon)^2} + \frac{-x^2U_\varepsilon}{\rho_g\varepsilon^2}\right]_{out} - \left[\frac{(1-x)^2U_\varepsilon}{\rho_l(1-\varepsilon)^2} + \frac{-x^2U_\varepsilon}{\rho_g\varepsilon^2}\right]_{in}\right\}\right)^2\right]^{1/2}$$

where $U_G = 12.35\%$ which is the highest obtained uncertainty for all mass fluxes calculated according to:

$$G = \frac{\dot{m}}{\pi\frac{d^2}{4}}$$

$$U_R = \left[\sum_{i=1}^{n}\left(\frac{\partial R}{\partial V_i} U_{V_i}\right)^2\right]^{\frac{1}{2}}$$

$$U_G = \left[\left(\frac{U_{\dot{m}}}{\pi\frac{d^2}{4}}\right)^2 + \left(-8\frac{\dot{m}}{\pi d^3} U_d\right)^2\right]^{1/2}$$

Calculation of uncertainty for all mass fluxes ($U_{\dot{m}} = 0.1\% \times \dot{m}$) is as the following:

$$U_{G=350} = \left[\left(\frac{0.001\times0.018}{\pi\frac{0.0081^2}{4}}\right)^2 + \left(-8\frac{0.018}{\pi\times0.0081^3} \times 0.0005\right)^2\right]^{1/2} = 43.21$$

$$\%U_G = \left(\frac{U_G}{G}\right) \times 100 = \frac{43.21}{350} \times 100 = 12.4\%$$

$$U_{G=300} = \left[\left(\frac{0.001\times0.015}{\pi\frac{0.0081^2}{4}}\right)^2 + \left(-8\frac{0.015}{\pi\times0.0081^3} \times 0.0005\right)^2\right]^{1/2} = 37.04$$

$$\%U_G = \left(\frac{U_G}{G}\right) \times 100 = \frac{37.04}{300} \times 100 = 12.4\%$$

$$U_{G=200} = \left[\left(\frac{0.001\times0.010}{\pi\frac{0.0081^2}{4}}\right)^2 + \left(-8\frac{0.010}{\pi\times0.0081^3}\times0.0005\right)^2\right]^{1/2} = 24.69$$

$$\%U_G = \left(\frac{U_G}{G}\right)\times100 = \frac{24.69}{200}\times100 = 12.4\%$$

$$U_{G=160} = \left[\left(\frac{0.001\times0.008}{\pi\frac{0.0081^2}{4}}\right)^2 + \left(-8\frac{0.008}{\pi\times0.0081^3}\times0.0005\right)^2\right]^{1/2} = 19.75$$

$$\%U_G = \left(\frac{U_G}{G}\right)\times100 = \frac{19.75}{160}\times100 = 12.4\%$$

and, $U_x = 5\%$ (The uncertainty of vapor quality from our previous paper [30]) referring to the other paper [9] of the same authors for the obtained formula:

$$U_x = \left\{\left[\frac{2\gamma I U_V}{\dot{m}_{ref}h_{fg,pe}}\right]^2 + \left[\frac{2\gamma V U_I}{\dot{m}_{ref}h_{fg,pe}}\right]^2 + \left[\frac{2\gamma VIU_{\dot{m}_{ref}}}{{\dot{m}_{ref}}^2h_{fg,pe}}\right]^2 + 2\left[\frac{C_pU_T}{h_{fg,pe}}\right]^2\right\}^{1/2}$$

U_ε can be calculated from Zivi's form of void fraction [26]. Therefore, after derivation, we have:

$$U_\varepsilon = \frac{U_x(\frac{\rho_g}{\rho_l})^{2/3}}{\left[1+\left(\frac{1-x_{te}}{x_{te}}\right)\left(\frac{\rho_g}{\rho_l}\right)^{\frac{2}{3}}\right]^2 {x_{te}}^2}$$

For all the datapoints, the uncertainty of void fraction was calculated. The highest uncertainty of $\%U_\varepsilon = 2.295$ obtained for a data point (related to the plain tube) with the lowest vapor quality for which the information is supplied in the table below:

Vapor quality	Mass flux ($kgm^{-2}s^{-1}$)	void fraction	Frictional Pressure Drop (kPa)	$\%U_\varepsilon$
0.106	300	0.589	2.387	2.29

By substituting the relevant uncertainties for each datapoint (i.e. U_G, U_x, and U_ε), all the momentum pressure drop uncertainties have been calculated. The highest percentage was $\%U_{\Delta P_{mom}} = 18.4$ which has an uncertainty of $U_{\Delta P_{mom}} = 0.07038\ \mathrm{kPa}$. This uncertainty occurred for the highest mass flux of 350 $kgm^{-2}s^{-1}$ at

vapor quality of $x = 0.25$ which has a $\Delta P_{fric} = 3.47784\ kPa$ and a $\Delta P_{mom} = 0.38215$ kPa. Therefore, by having the total pressure drop reading of $\Delta P_{tot} = 3.86\ kPa$ (from the differential pressure transmitter with an accuracy of 0.075% of reading) $U_{\Delta P_{tot}} = 0.00075 \times 3.86$. And, $U_{\Delta P_{mom}} = 0.07038$ kPa. Thus, the highest possible uncertainty for frictional pressure drop is:

$$U_{\Delta P_{fric}} = \left[\left(U_{\Delta P_{tot}}\right)^2 + \left(U_{\Delta P_{mom}}\right)^2\right]^{1/2} = [(0.00075 \times 3.86)^2 + (0.07038)^2]^{1/2} = 0.07045 \text{ kPa}$$

$$\%U_{\Delta P_{fric}} = \left(\frac{U_{\Delta P_{fric}}}{\Delta P_{fric}}\right) \times 100 = \frac{0.07045}{3.47784} \times 100 = 2.85\ \%$$

To assess the uncertainty of PF, we have:

$$PF = {R_{HTC}}/{R_{\Delta P}} = \frac{{HTC_r}/{HTC_p}}{{(\Delta P)_r}/{(\Delta P)_p}} \quad (1)$$

where $HTC_r = 6296.84$ $Wm^{-2}K^{-1}$, $HTC_p = 4271.36$ $Wm^{-2}K^{-1}$, $\Delta P_r = 5.94$ kPa, and $\Delta P_p = 4.04$ kPa. (These values were calculated from the performance factor of 1.0 for TT2 at G = 300 $kgm^{-2}s^{-1}$ in the experiments, as shown in Fig. 6 in the paper)

According to Schultz and Cole [27], we have:

$$U_{PF} = \left[\left(\frac{1}{\frac{HTC_p}{\frac{\Delta P_r}{\Delta P_p}}} U_{HTC_r}\right)^2 + \left(\frac{\frac{-HTC_r}{{HTC_p}^2}}{\frac{\Delta P_r}{\Delta P_p}} U_{HTC_p}\right)^2 + \left(\frac{\frac{-HTC_r}{\Delta P_p HTC_p}}{\left(\frac{\Delta P_r}{\Delta P_p}\right)^2} U_{\Delta P_r}\right)^2 + \left(\frac{\frac{-HTC_r \Delta P_r}{{\Delta P_p}^2 HTC_p}}{\left(\frac{\Delta P_r}{\Delta P_p}\right)^2} U_{\Delta P_p}\right)^2\right]^{1/2}$$

Based on the test rig and measurement uncertainties in the Table 4, we have:

$U_{HTC_r} = 0.08 \times 6296.84$ = 503.75 $Wm^{-2}K^{-1}$, $U_{HTC_p} = 0.08 \times 4271.36$ = 341.71 $Wm^{-2}K^{-1}$, $U_{\Delta P_r} = 0.0285 \times 5.94$ = 0.169 kPa, and $U_{\Delta P_p} = 0.0285 \times 4.04$ = 0.115

kPa. By substituting the uncertainties into the derived uncertainty for performance factor, we have:

$$U_{PF=1.0} = [(0.08)^2 + (-0.08)^2 + (-0.029)^2 + (-0.029)^2]^{1/2} = 0.043$$

And therefore the % uncertainty is:

$$\%U_{PF=1.0} = \frac{0.043}{1.0} \times 100 = \pm 4.3\ \%$$

8. References

[1] D. Calleja-Anta, L. Nebot-Andrés, J. Catalán-Gil, D. Sánchez, R. Cabello, and R. Llopis, "Thermodynamic screening of alternative refrigerants for R290 and R600a," *Results in Engineering,* vol. 5, p. 100081, 2020.

[2] H. A. Moghaddam, M. Shafaee, and R. Riazi, "Numerical investigation of a refrigeration ejector: effects of environment-friendly refrigerants and geometry of the ejector mixing chamber," *European Journal of Sustainable Development Research,* vol. 3, no. 3, p. em0090, 2019.

[3] M. Ahmadpour and M. Akhavan-Behabadi, "Experimental investigation of heat transfer during flow condensation of HC-R600a based nano-refrigerant inside a horizontal U-shaped tube," *International Journal of Thermal Sciences,* vol. 146, p. 106110, 2019.

[4] J. Copetti, M. Macagnan, and F. Zinani, "Experimental study on R-600a boiling in 2.6 mm tube," *international journal of refrigeration,* vol. 36, no. 2, pp. 325-334, 2013.

[5] D. F. Sempértegui-Tapia and G. Ribatski, "Flow boiling heat transfer of R134a and low GWP refrigerants in a horizontal micro-scale channel," *International Journal of Heat and Mass Transfer,* vol. 108, pp. 2417-2432, 2017.

[6] M. Shafaee, F. Alimardani, and S. Mohseni, "An empirical study on evaporation heat transfer characteristics and flow pattern visualization in tubes with coiled wire inserts," *International Communications in Heat and Mass Transfer,* vol. 76, pp. 301-307, 2016.

[7] M. Shafaee, H. Mashouf, A. Sarmadian, and S. Mohseni, "Evaporation heat transfer and pressure drop characteristics of R-600a in horizontal smooth and helically dimpled tubes," *Applied Thermal Engineering,* vol. 107, pp. 28-36, 2016.

[8] A. Sarmadian, M. Shafaee, H. Mashouf, and S. Mohseni, "Condensation heat transfer and pressure drop characteristics of R-600a in horizontal smooth and helically dimpled tubes," *Experimental Thermal and Fluid Science,* vol. 86, pp. 54-62, 2017.

[9] H. Mashouf, M. Shafaee, A. Sarmadian, and S. Mohseni, "Visual study of flow patterns during evaporation and condensation of R-600a inside horizontal smooth and helically dimpled tubes," *Applied Thermal Engineering,* vol. 124, pp. 1392-1400, 2017.

[10] Z.-Q. Yang, G.-F. Chen, Y. Yao, Q.-L. Song, J. Shen, and M.-Q. Gong, "Experimental study on flow boiling heat transfer and pressure drop in a horizontal tube for R1234ze (E) versus R600a," *International Journal of Refrigeration,* vol. 85, pp. 334-352, 2018.

[11] H. A. Moghaddam, A. Sarmadian, and M. Shafaee, "An experimental study on condensation heat transfer characteristics of R-600a in tubes with coiled wire inserts," *Applied Thermal Engineering,* vol. 159, p. 113889, 2019.

[12] H. A. Moghaddam, A. Sarmadian, M. Shafaee, and H. Enayatollahi, "Flow pattern maps, pressure drop and performance assessment of horizontal tubes with coiled wire inserts during condensation of R-600a," *International Journal of Heat and Mass Transfer,* vol. 148, p. 119062, 2020.
[13] F. T. Kanizawa, T. S. Mogaji, and G. Ribatski, "Evaluation of the heat transfer enhancement and pressure drop penalty during flow boiling inside tubes containing twisted tape insert," *Applied thermal engineering,* vol. 70, no. 1, pp. 328-340, 2014.
[14] A. Shishkin, F. T. Kanizawa, G. Ribatski, S. Tarasevich, and A. Yakovlev, "Experimental investigation of the heat transfer coefficient during convective boiling of R134a in tubes with twisted tape insert," *International Journal of Refrigeration,* vol. 92, pp. 196-207, 2018.
[15] M. Akhavan-Behabadi, R. Kumar, and M. Jamali, "Investigation on heat transfer and pressure drop during swirl flow boiling of R-134a in a horizontal tube," *International Journal of Heat and Mass Transfer,* vol. 52, no. 7-8, pp. 1918-1927, 2009.
[16] V. Hejazi, M. Akhavan-Behabadi, and A. Afshari, "Experimental investigation of twisted tape inserts performance on condensation heat transfer enhancement and pressure drop," *International Communications in Heat and Mass Transfer,* vol. 37, no. 9, pp. 1376-1387, 2010.
[17] M. Salimpour and S. Yarmohammadi, "Effect of twisted tape inserts on pressure drop during R-404A condensation," *International journal of refrigeration,* vol. 35, no. 2, pp. 263-269, 2012.
[18] M. Salimpour and S. Yarmohammadi, "Heat transfer enhancement during R-404A vapor condensation in swirling flow," *International journal of refrigeration,* vol. 35, no. 7, pp. 2014-2021, 2012.
[19] H. A. Moghaddam *et al.*, "Condensation heat transfer and pressure drop characteristics of Isobutane in horizontal channels with twisted tape inserts," *International Journal of Refrigeration,* 2020.
[20] A. Kumar, R. Datt, M. Singh Bhist, A. Darshan Kothiyal, and R. Maithani, "HYDRODYNAMIC AND THERMAL PERFORMANCE TWISTED TAPE INSERT PROVIDED IN HEAT EXCHANGER TUBES: A REVIEW," *Frontiers in Heat and Mass Transfer (FHMT),* vol. 12, 2018.
[21] H. Bucak and F. Yilmaz, "The Current State on the Thermal Performance of Twisted Tapes: A Geometrical Categorisation Approach," *Chemical Engineering and Processing-Process Intensification,* p. 107929, 2020.
[22] A. Dewan, P. Mahanta, K. S. Raju, and P. S. Kumar, "Review of passive heat transfer augmentation techniques," *Proceedings of the Institution of Mechanical Engineers, Part A: Journal of Power and Energy,* vol. 218, no. 7, pp. 509-527, 2004.
[23] S. Liu and M. Sakr, "A comprehensive review on passive heat transfer enhancements in pipe exchangers," *Renewable and sustainable energy reviews,* vol. 19, pp. 64-81, 2013.
[24] M. Garg, H. Nautiyal, S. Khurana, and M. Shukla, "Heat transfer augmentation using twisted tape inserts: A review," *Renewable and Sustainable Energy Reviews,* vol. 63, pp. 193-225, 2016.
[25] J. G. Collier and J. R. Thome, *Convective boiling and condensation*. Clarendon Press, 1994.
[26] S. Zivi, "Estimation of steady-state steam void-fraction by means of the principle of minimum entropy production," 1964.
[27] R. Schultz and S. RR, "Uncertainty analysis in boiling nucleation," 1979.
[28] K. Agrawal and H. Varma, "Experimental study of heat transfer augmentation versus pumping power in a horizontal R12 evaporator," *International journal of refrigeration,* vol. 14, no. 5, pp. 273-281, 1991.
[29] N. Kattan, J. R. Thome, and D. Favrat, "Flow boiling in horizontal tubes: part 3—development of a new heat transfer model based on flow pattern," 1998.

[30] F. Alimardani, H. A. Moghaddam, A. Sarmadian, and M. Shafaee, "Pressure loss and performance assessment of horizontal spiral coil inserted pipes during forced convective evaporation of R-600a," *International Journal of Refrigeration,* vol. 107, pp. 20-30, 2019.
[31] L. Friedel, "Improved friction pressure drop correlation for horizontal and vertical two-phase pipe flow," *Proc. of European Two-Phase Flow Group Meet., Ispra, Italy, 1979,* 1979.
[32] H. Müller-Steinhagen and K. Heck, "A simple friction pressure drop correlation for two-phase flow in pipes," *Chemical Engineering and Processing: Process Intensification,* vol. 20, no. 6, pp. 297-308, 1986.
[33] T. Naulboonrueng, J. Kaewon, and S. Wongwises, "Two-phase condensation heat transfer coefficients of HFC–134a at high mass flux in smooth and micro-fin tubes," *International communications in heat and mass transfer,* vol. 30, no. 4, pp. 577-590, 2003.
[34] M. Macdonald and S. Garimella, "Hydrocarbon condensation in horizontal smooth tubes: Part I–Measurements," *International Journal of Heat and Mass Transfer,* vol. 93, pp. 75-85, 2016.